X-ray Emission from High-Redshift Star-Forming Galaxies: Results from the 4 Ms Chandra Deep Field South (CDF-S) Survey

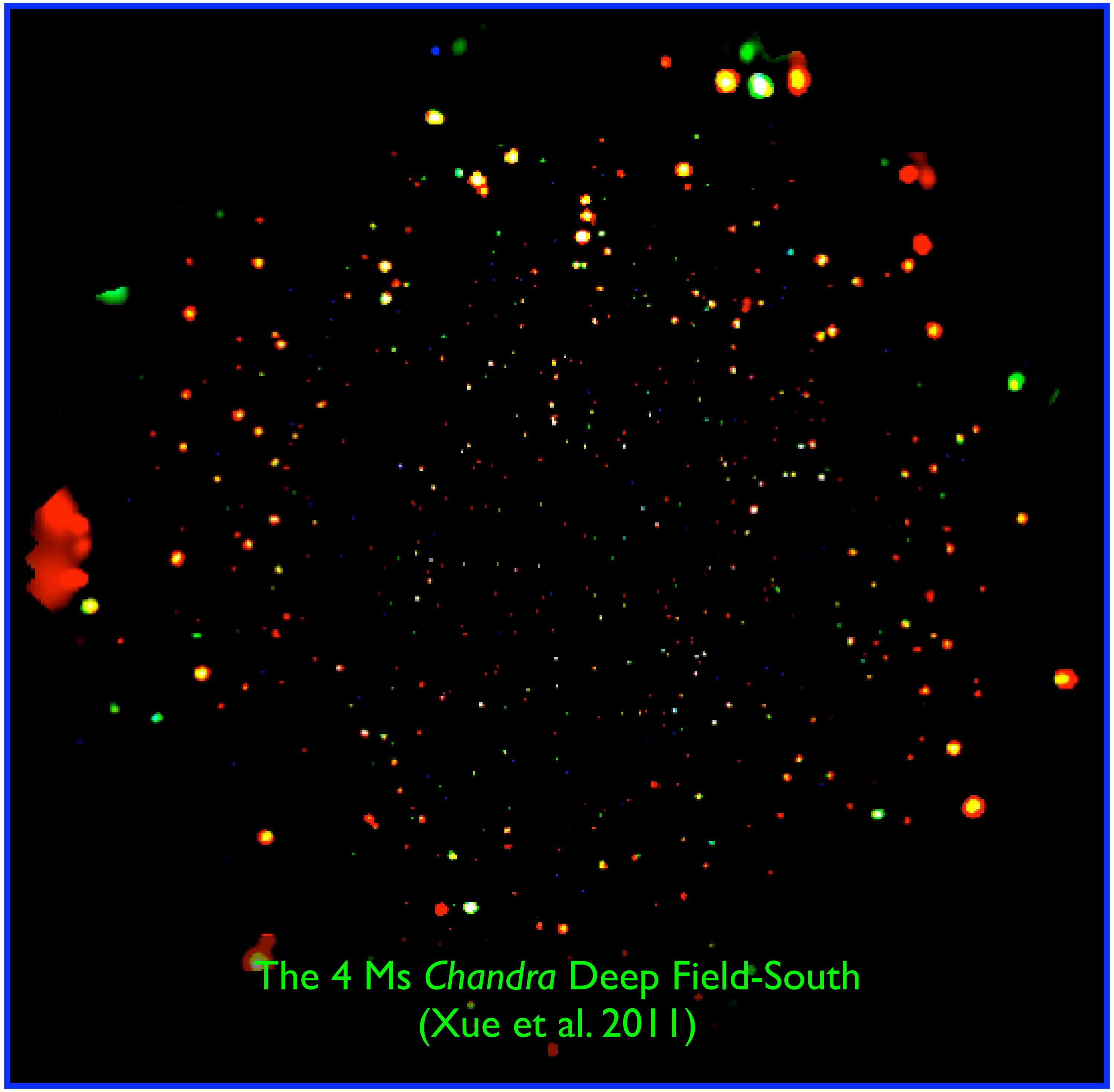

Bret Lehmer
(Johns Hopkins/Goddard)
Einstein Fellow

Antara Basu-Zych
Niel Brandt
Ann Hornschemeier
Bin Luo
Yongquan Xue
Dave Alexander
Franz Bauer
Tassos Fragos
Leigh Jenkins
Vicky Kalogera
Andy Ptak
Andreas Zezas

X-ray Emission from High-Redshift Star-Forming Galaxies: Results from the 4 Ms Chandra Deep Field South (CDF-S) Survey

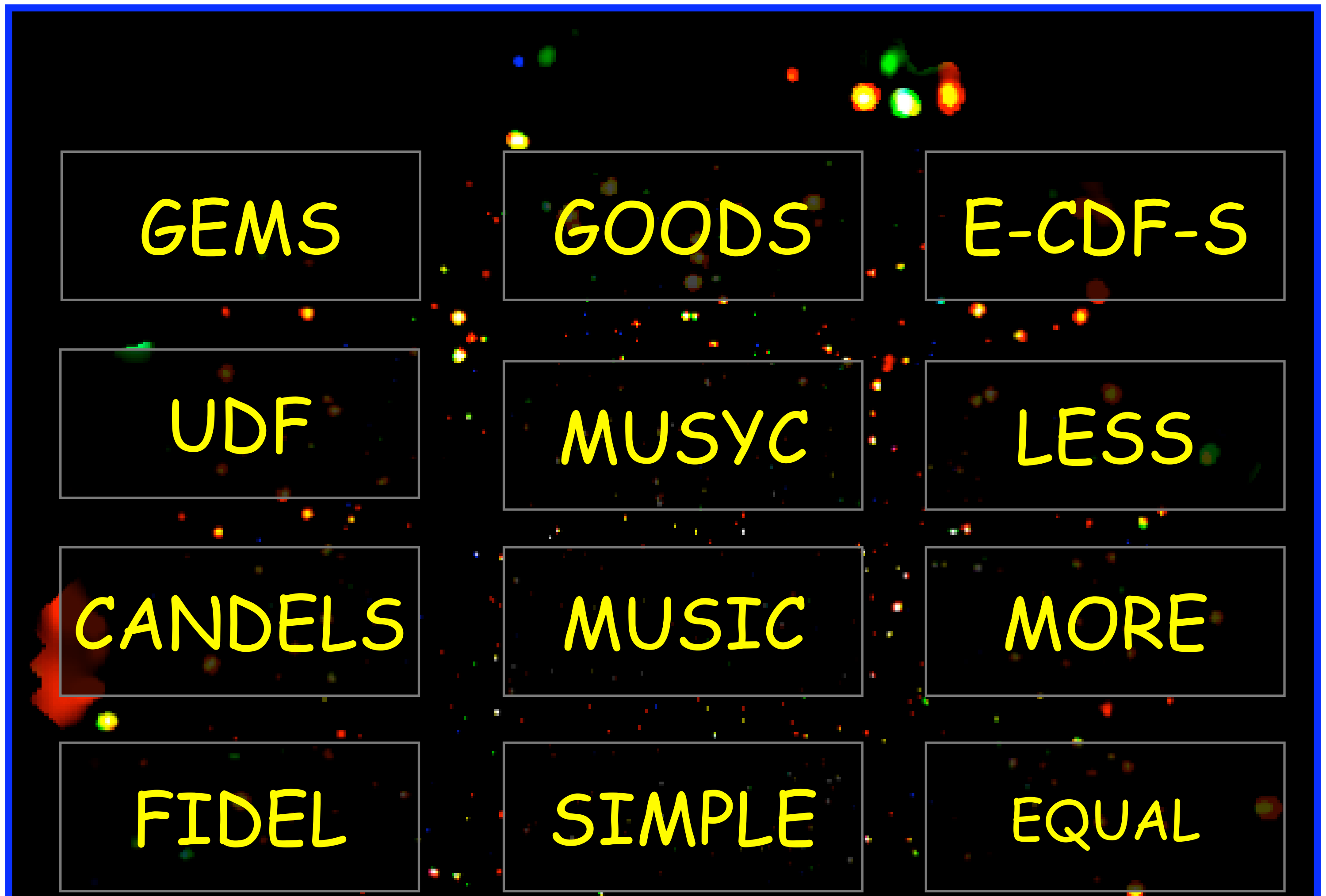

Bret Lehmer
(Johns Hopkins/Goddard)
Einstein Fellow

Antara Basu-Zych
Niel Brandt
Ann Hornschemeier
Bin Luo
Yongquan Xue
Dave Alexander
Franz Bauer
Tassos Fragos
Leigh Jenkins
Vicky Kalogera
Andy Ptak
Andreas Zezas

X-ray Counts: The Rise of Normal Galaxies

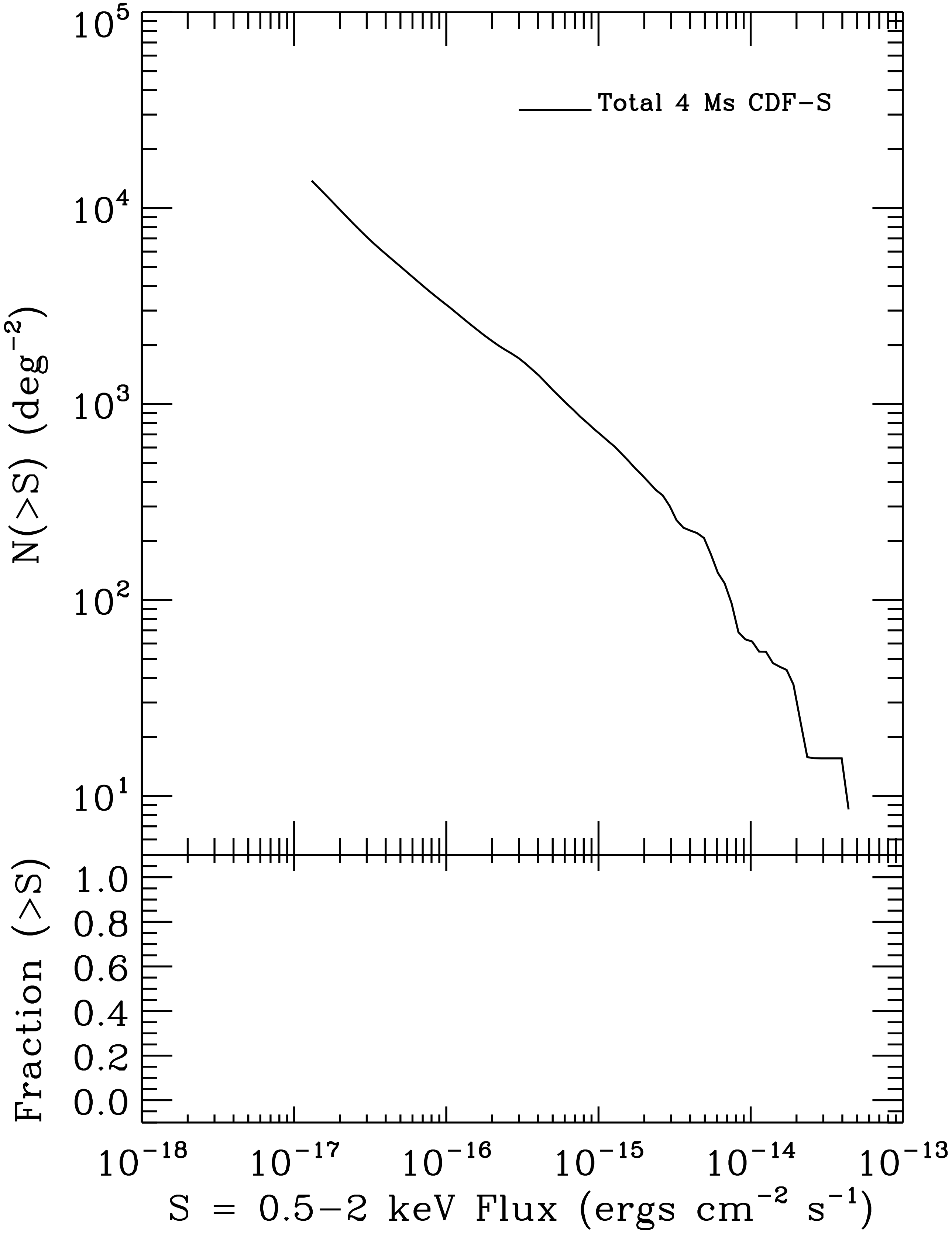

- 740 total X-ray sources are detected across the field.
- Reach 0.5−2 keV flux limit of 1.1×10^{-17} ergs cm^{-2} s^{-1} and source densities of over 14,000 deg^{-2}.
- Broadly classified sources as
  - − AGNs (556)—broad emission lines, hard X-ray spectra, large X-ray-to-optical ratios, powerful radio sources.
  - − Normal galaxies (174)—small X-ray-to-optical flux ratios, steep power-law X-ray spectra.
  - − Galactic stars (10)—Stellar optical spectra, bright optical counterparts with small X-ray-to-optical flux ratios.
- Normal galaxies quickly rise at faintest flux levels and make up ~40% of the cumulative number counts.

Lehmer et al. (2011)

X-ray Counts: The Rise of Normal Galaxies

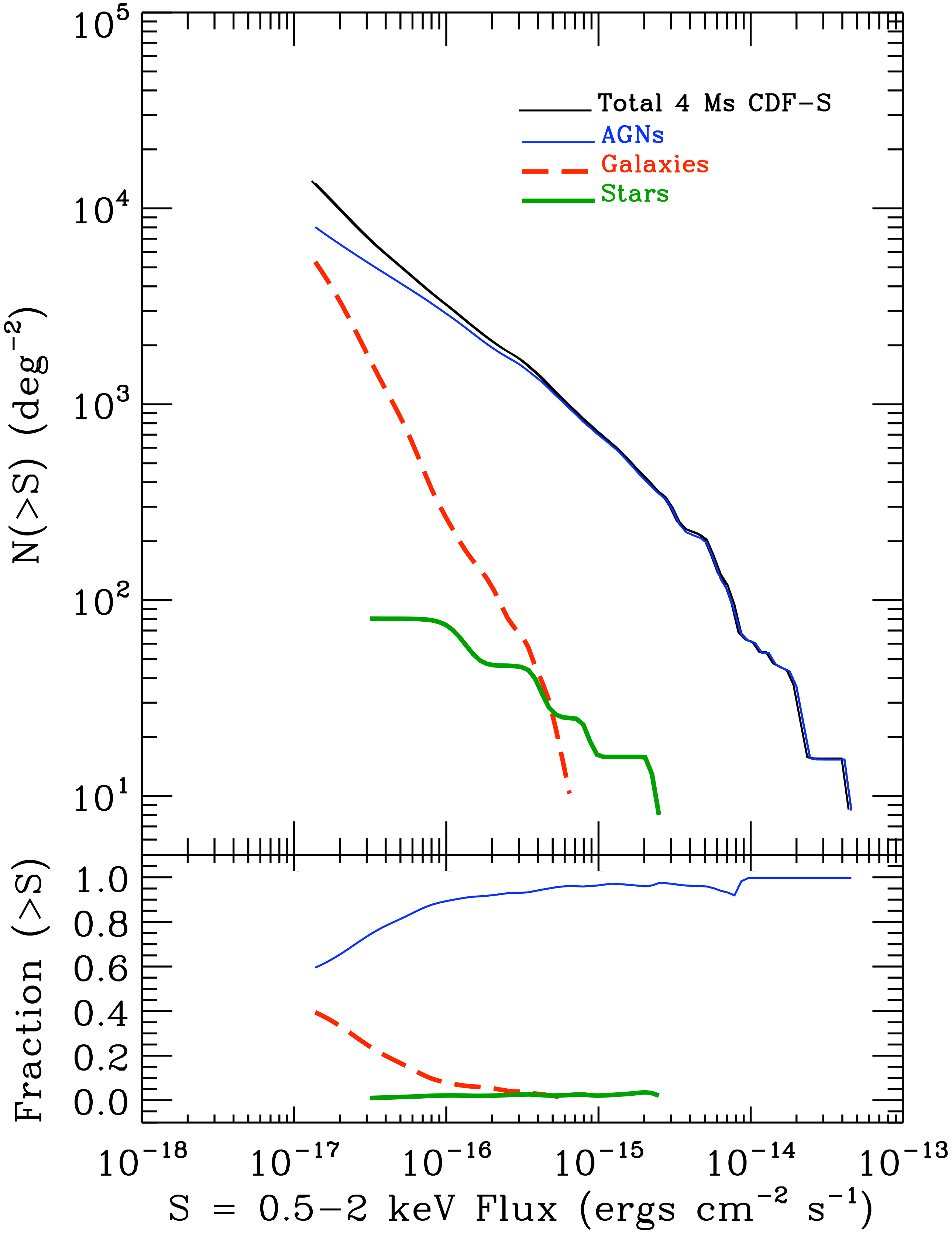

- 740 total X-ray sources are detected across the field.
- Reach 0.5−2 keV flux limit of 1.1×10^{-17} ergs cm^{-2} s^{-1} and source densities of over 14,000 deg^{-2}.
- Broadly classified sources as
  - AGNs (556)—broad emission lines, hard X-ray spectra, large X-ray-to-optical ratios, powerful radio sources.
  - Normal galaxies (174)—small X-ray-to-optical flux ratios, steep power-law X-ray spectra.
  - Galactic stars (10)—Stellar optical spectra, bright optical counterparts with small X-ray-to-optical flux ratios.
- Normal galaxies quickly rise at faintest flux levels and make up ~40% of the cumulative number counts.

Lehmer et al. (2011)

Morphological Breakdown of Number Counts

- Using *HST* imaging and galaxy color, we classified the 174 galaxies as late-type star-forming galaxies (135) or early-type passive galaxies (39).
- Variety of galaxies detected over the redshift range $z = 0{-}1.6$.

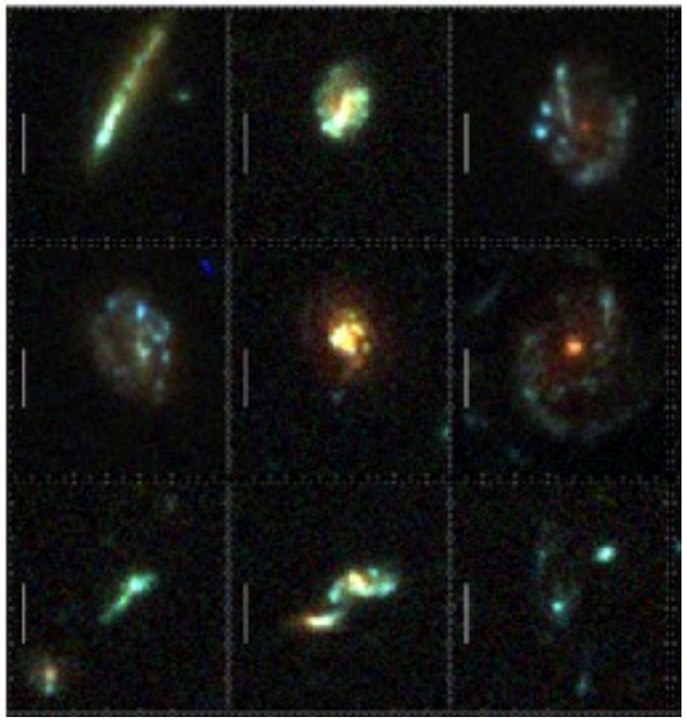

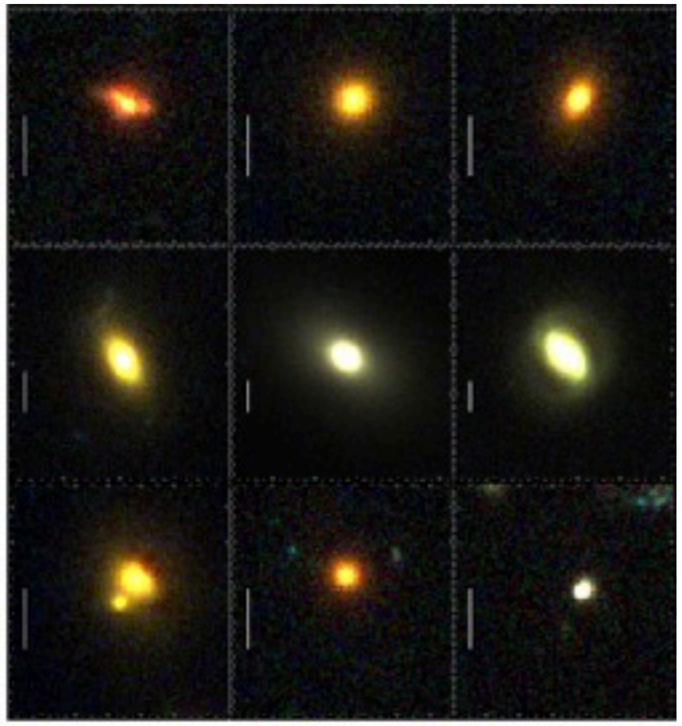

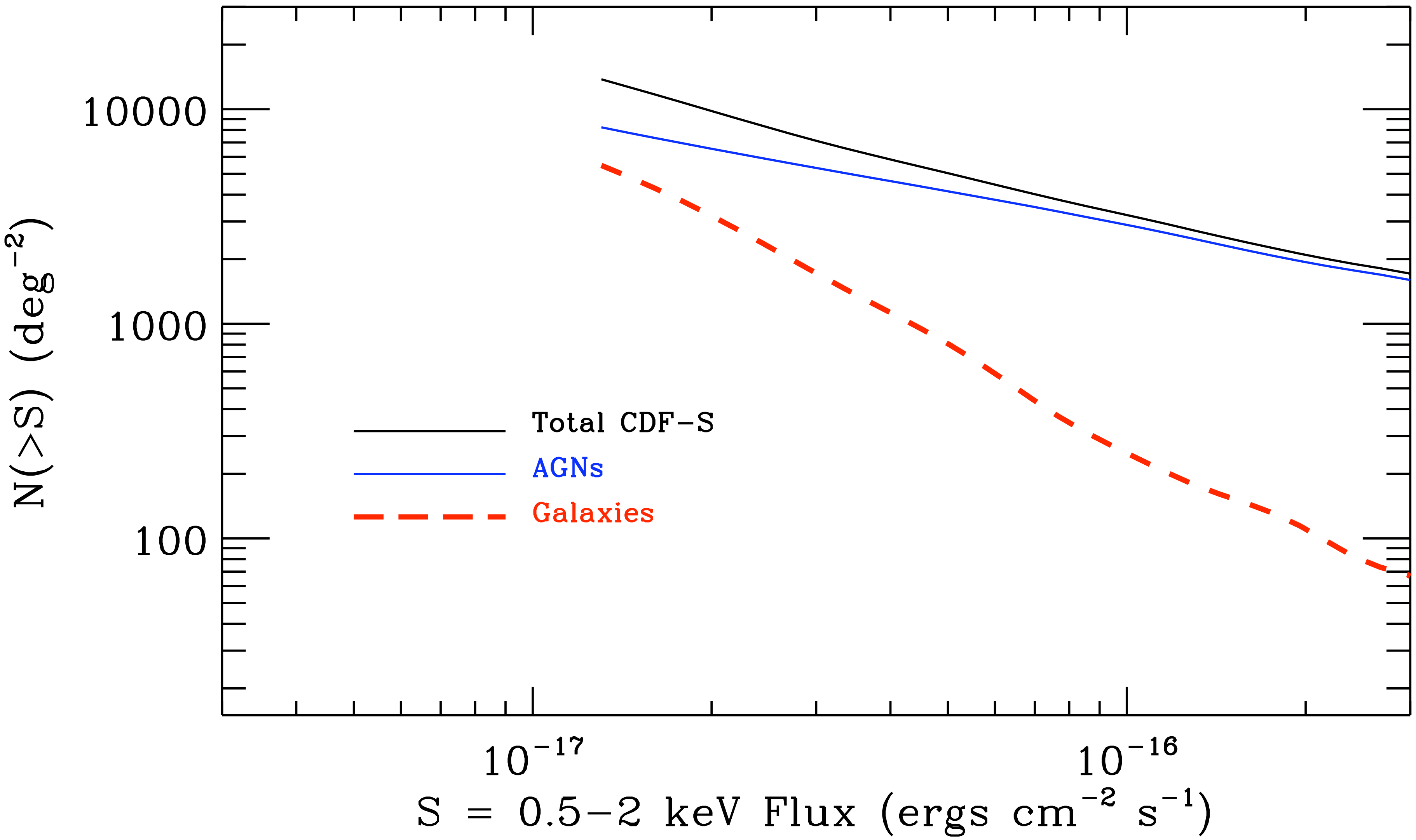

Morphological Breakdown of Number Counts

- Using *HST* imaging and galaxy color, we classified the 174 galaxies as late-type star-forming galaxies (135) or early-type passive galaxies (39).
- Variety of galaxies detected over the redshift range $z = 0-1.6$.

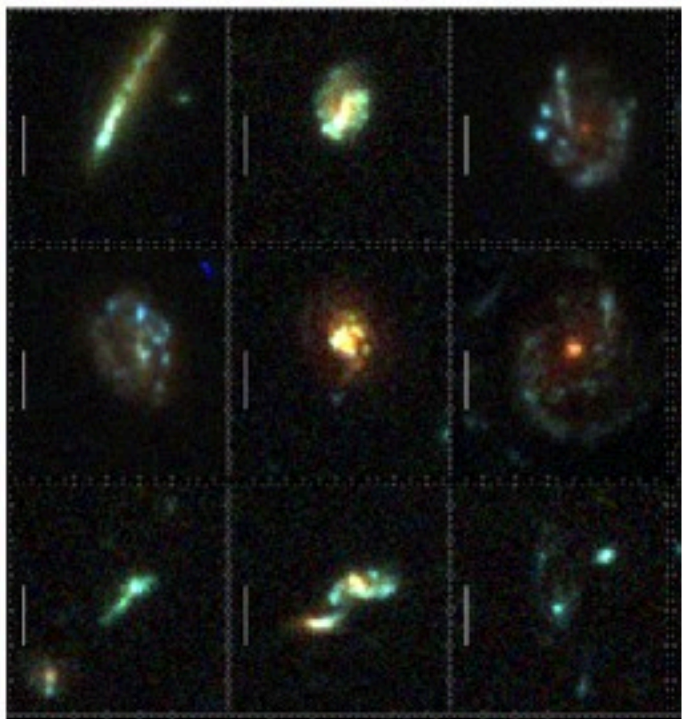

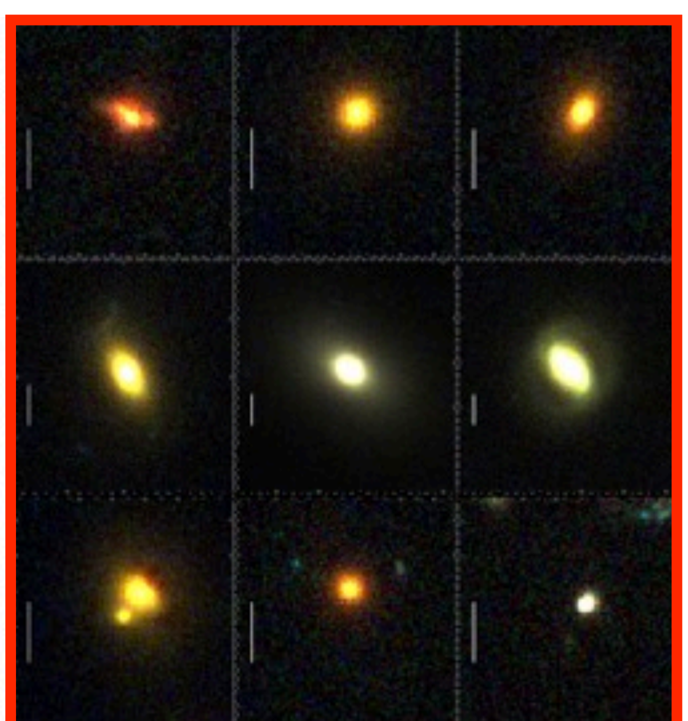

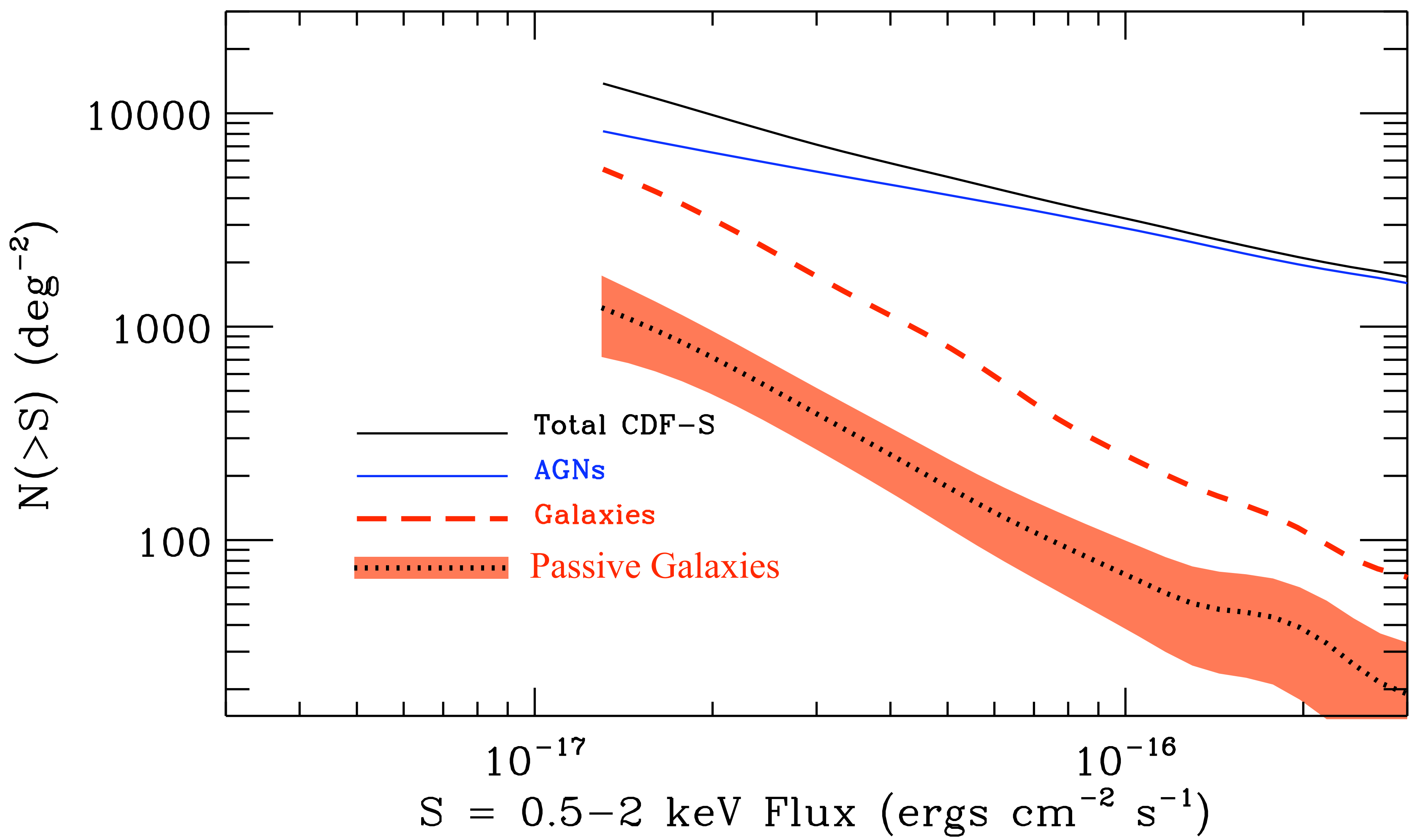

Morphological Breakdown of Number Counts

- Using *HST* imaging and galaxy color, we classified the 174 galaxies as late-type star-forming galaxies (135) or early-type passive galaxies (39).
- Variety of galaxies detected over the redshift range $z = 0-1.6$.

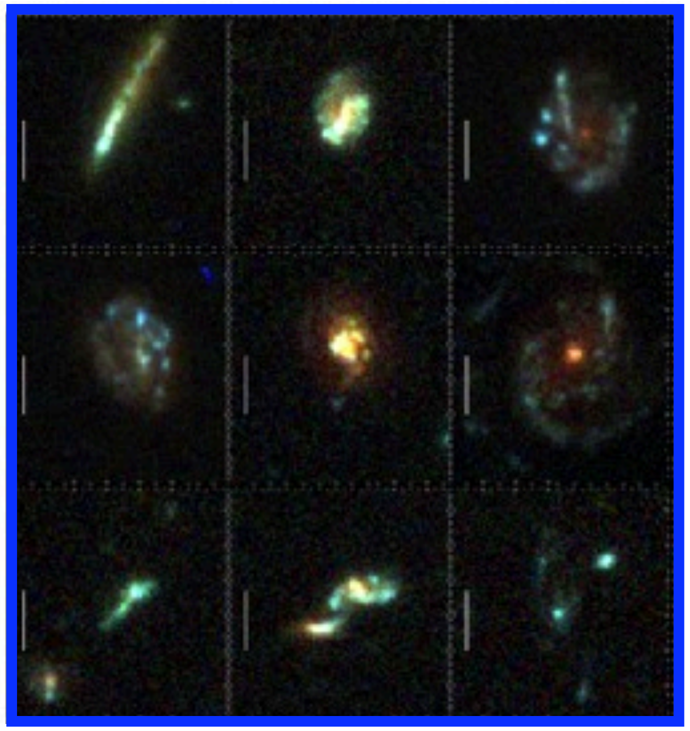

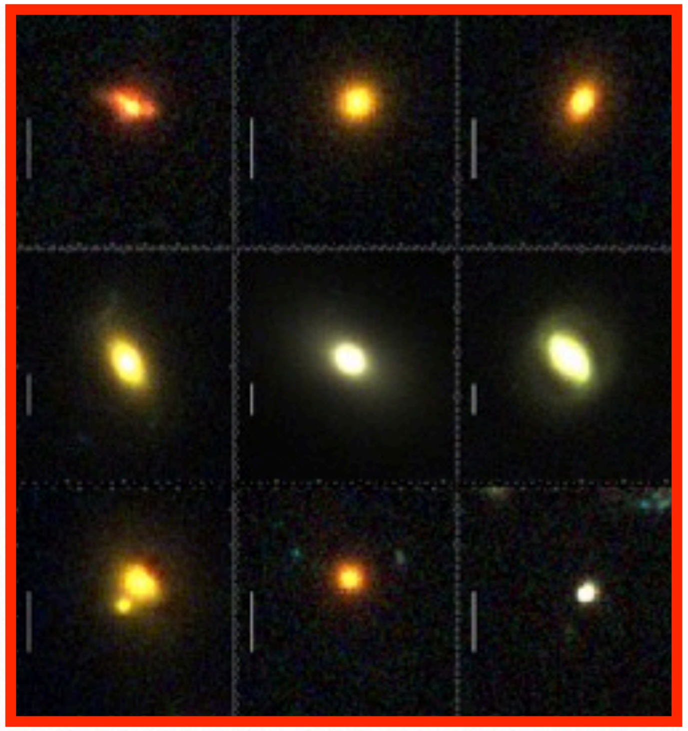

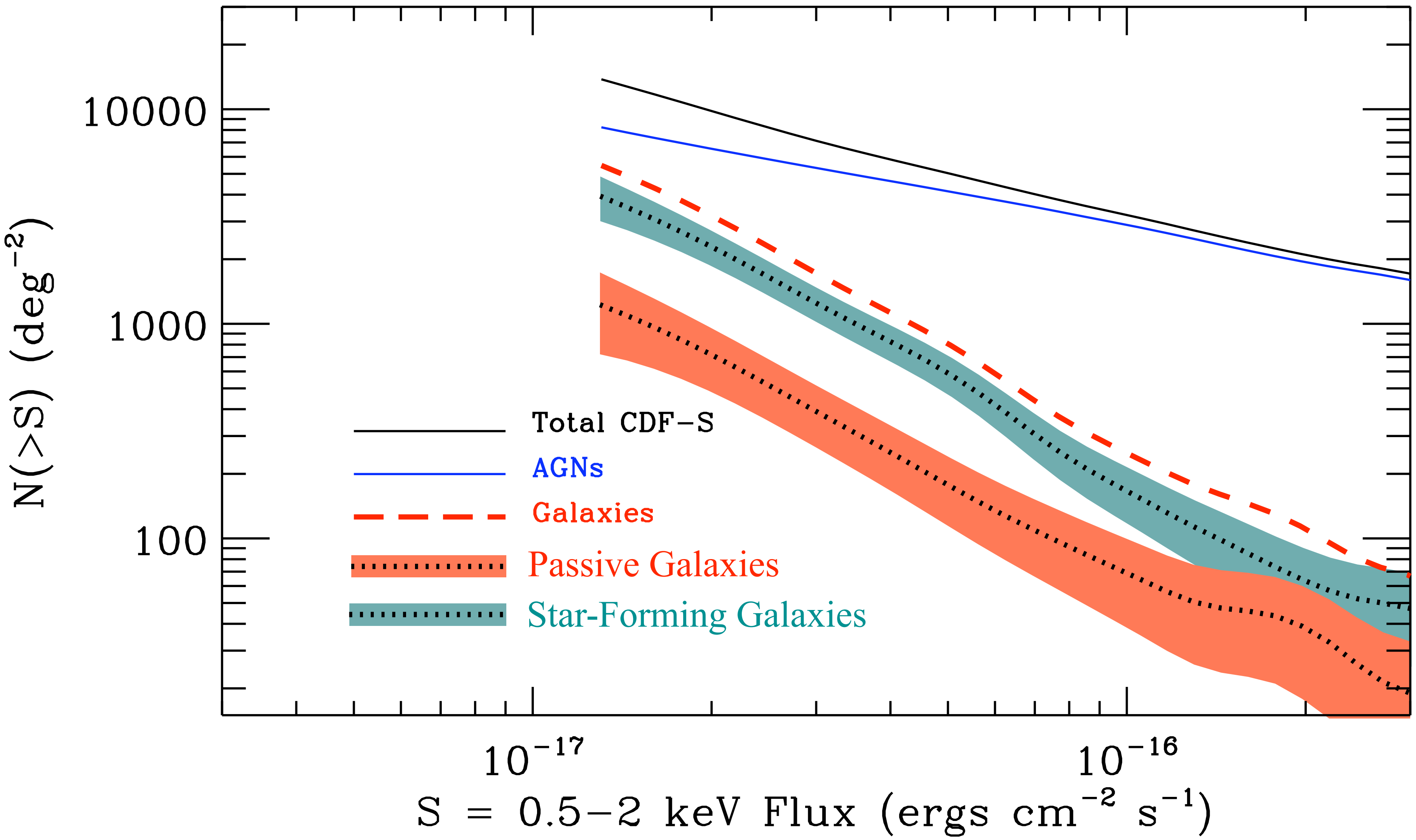

What Does This Rise In SF Galaxy Counts Tell Us About Galaxy Evolution?

- X-ray number counts for star-forming galaxies can be modeled using the X-ray luminosity function (XLF) and its redshift evolution.

$$N(>S_{\rm X}) = \frac{1}{\Omega_{\rm sky}} \int_{\infty}^{S_{\rm X}} \left(\int_0^{\infty} \frac{dN}{dL_{\rm X} dV} \frac{dL_{\rm X}}{dS_{\rm X}} \frac{dV}{dz} dz \right) dS_{\rm X}$$

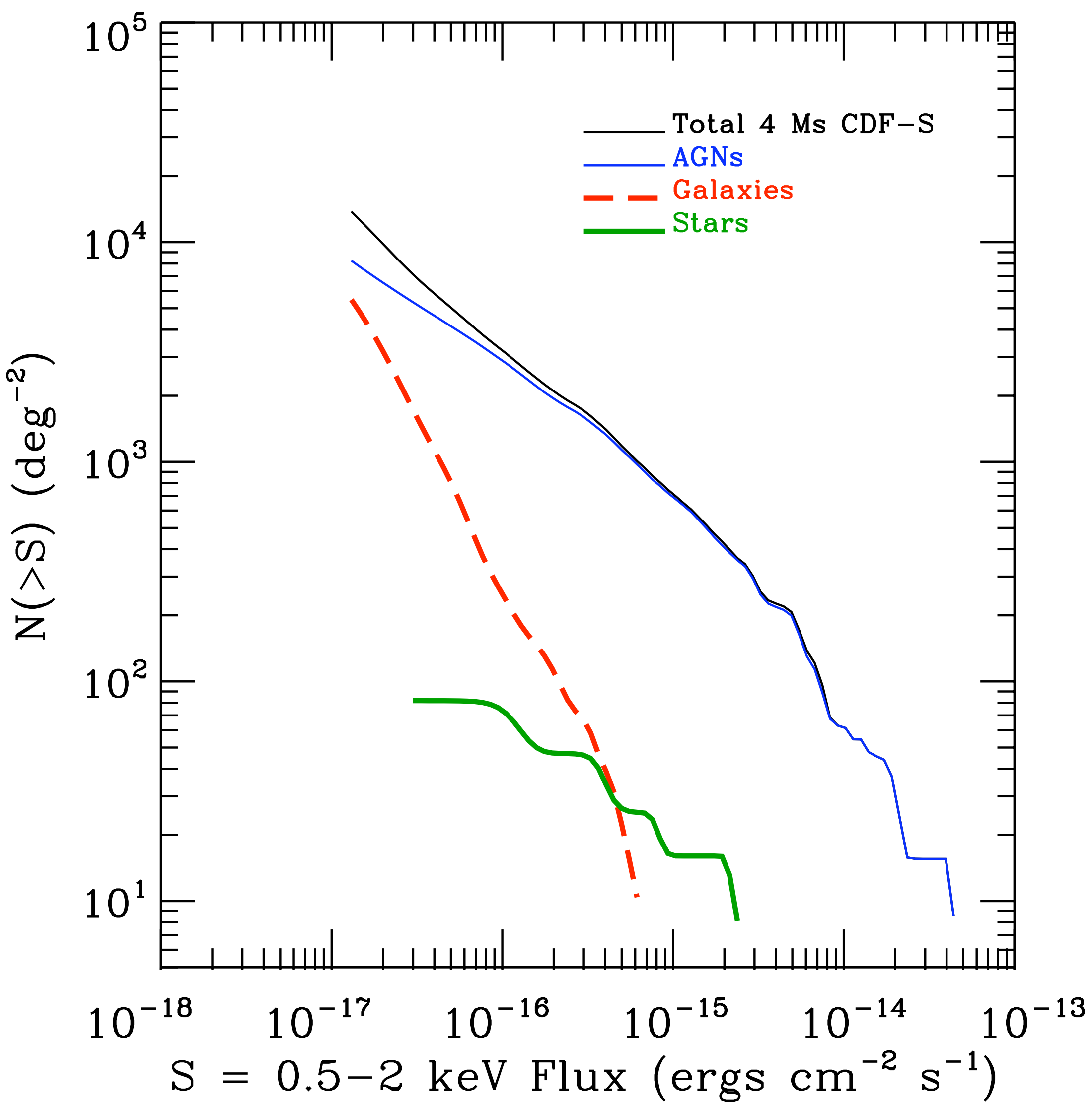

$\frac{dV}{dz}$ → $$\frac{c}{H_0} \frac{(1+z)^2 d_A^2}{[\Omega_\Lambda + (1+z)^3 \Omega_m]^{1/2}}$$

$\frac{dL_{\rm X}}{dS_{\rm X}}$ → $$4\pi d_L^2 K(z)$$

$\frac{dN}{dL_{\rm X} dV}$ → Redshift Evolution of the X-ray Luminosity Function ????

Cosmic Evolution of X-ray Luminosity Function for Star-Forming Galaxies

- Evolution of X-ray luminosity function (XLF) can be directly constrained for most X-ray luminous galaxies to $z \sim 1$ using the X-ray detected sources (e.g., Norman+2004; Ptak+2007; Tzanavaris+2008).

- Want to understand rise in the X-ray number counts in the context of the cosmic evolution of the galaxy properties (e.g., stellar mass and SFR).

$$N(>S_{\rm X}) = \frac{1}{\Omega_{\rm sky}} \int_{\infty}^{S_{\rm X}} \left(\int_0^{\infty} \boxed{\frac{dN}{dL_{\rm X} dV}} \frac{dL_{\rm X}}{dS_{\rm X}} \frac{dV}{dz} dz \right) dS_{\rm X}$$

$$\frac{dN}{dL_{\rm X} dV} = \frac{dN}{dM_\star dV} \frac{dM_\star}{d{\rm SFR}} \frac{d{\rm SFR}}{dL_{\rm X}}$$

Cosmic Evolution of X-ray Luminosity Function for Star-Forming Galaxies

- Evolution of X-ray luminosity function (XLF) can be directly constrained for most X-ray luminous galaxies to $z \sim 1$ using the X-ray detected sources (e.g., Norman+2004; Ptak+2007; Tzanavaris+2008).

- Want to understand rise in the X-ray number counts in the context of the cosmic evolution of the galaxy properties (e.g., stellar mass and SFR).

$$N(>S_X) = \frac{1}{\Omega_{sky}} \int_{\infty}^{S_X} \left(\int_0^{\infty} \boxed{\frac{dN}{dL_X dV}} \frac{dL_X}{dS_X} \frac{dV}{dz} dz \right) dS_X$$

$$\frac{dN}{dL_X dV} = \boxed{\frac{dN}{dM_\star dV}} \frac{dM_\star}{d\mathrm{SFR}} \frac{d\mathrm{SFR}}{dL_X}$$

Stellar Mass Function

Cosmic Evolution of X-ray Luminosity Function for Star-Forming Galaxies

- Evolution of X-ray luminosity function (XLF) can be directly constrained for most X-ray luminous galaxies to $z \sim 1$ using the X-ray detected sources (e.g., Norman+2004; Ptak+2007; Tzanavaris+2008).

- Want to understand rise in the X-ray number counts in the context of the cosmic evolution of the galaxy properties (e.g., stellar mass and SFR).

$$N(>S_{\rm X}) = \frac{1}{\Omega_{\rm sky}} \int_{\infty}^{S_{\rm X}} \left(\int_0^{\infty} \boxed{\frac{dN}{dL_{\rm X} dV}} \frac{dL_{\rm X}}{dS_{\rm X}} \frac{dV}{dz} dz \right) dS_{\rm X}$$

$$\frac{dN}{dL_{\rm X} dV} = \boxed{\frac{dN}{dM_\star dV}} \boxed{\frac{dM_\star}{d{\rm SFR}}} \frac{d{\rm SFR}}{dL_{\rm X}}$$

Stellar Mass Function

Relation Between Mass and SFR

Cosmic Evolution of X-ray Luminosity Function for Star-Forming Galaxies

- Evolution of X-ray luminosity function (XLF) can be directly constrained for most X-ray luminous galaxies to $z \sim 1$ using the X-ray detected sources (e.g., Norman+2004; Ptak+2007; Tzanavaris+2008).
- Want to understand rise in the X-ray number counts in the context of the cosmic evolution of the galaxy properties (e.g., stellar mass and SFR).

$$N(>S_{\rm X}) = \frac{1}{\Omega_{\rm sky}} \int_{\infty}^{S_{\rm X}} \left(\int_0^{\infty} \boxed{\frac{dN}{dL_{\rm X} dV}} \frac{dL_{\rm X}}{dS_{\rm X}} \frac{dV}{dz} dz \right) dS_{\rm X}$$

$$\frac{dN}{dL_{\rm X} dV} = \boxed{\frac{dN}{dM_\star dV}} \boxed{\frac{dM_\star}{d{\rm SFR}}} \boxed{\frac{d{\rm SFR}}{dL_{\rm X}}}$$

Stellar Mass Function

Relation Between Mass and SFR

X-ray/SFR Correlation

Cosmic Evolution of Star-Forming Galaxy Population

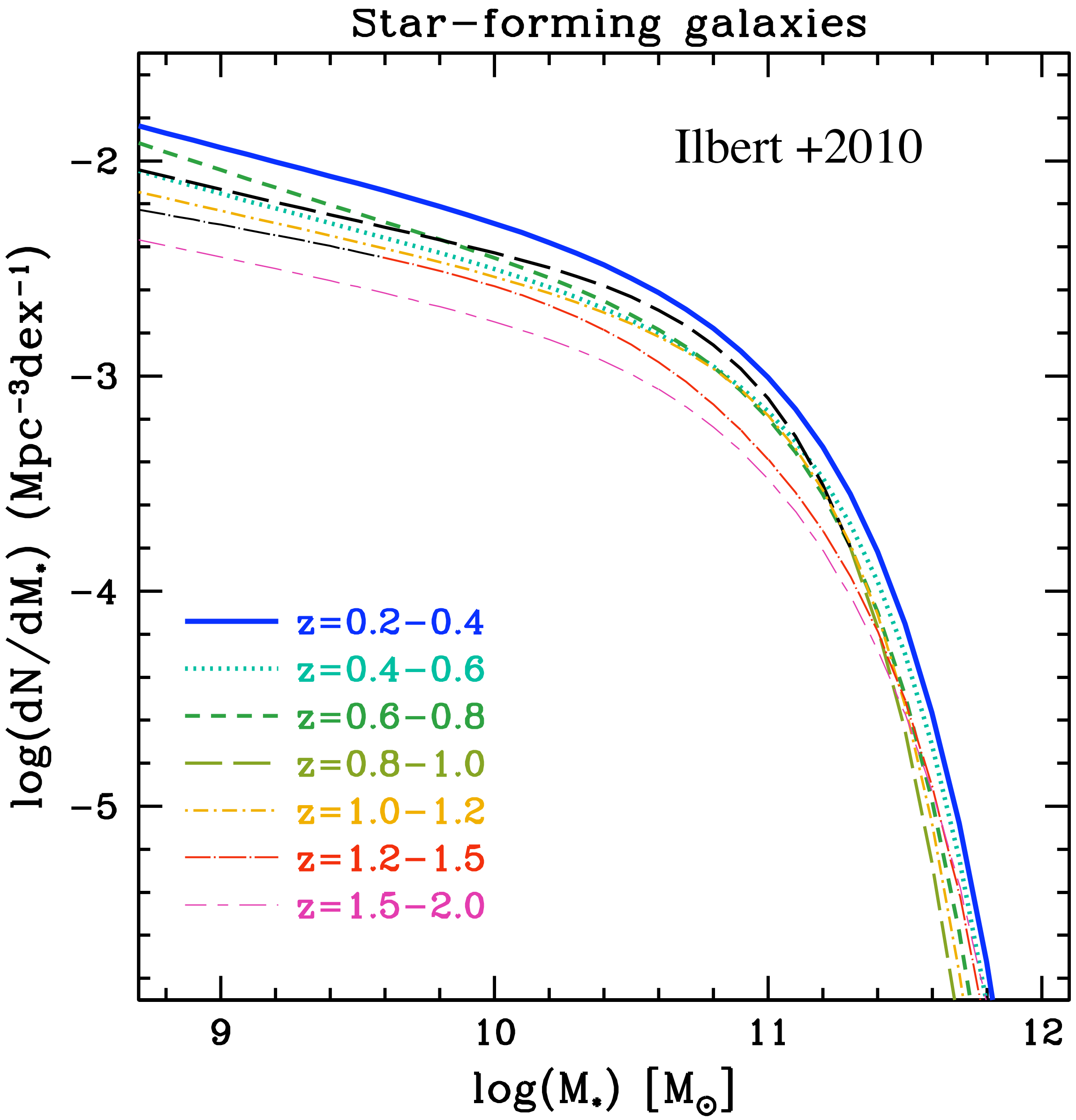

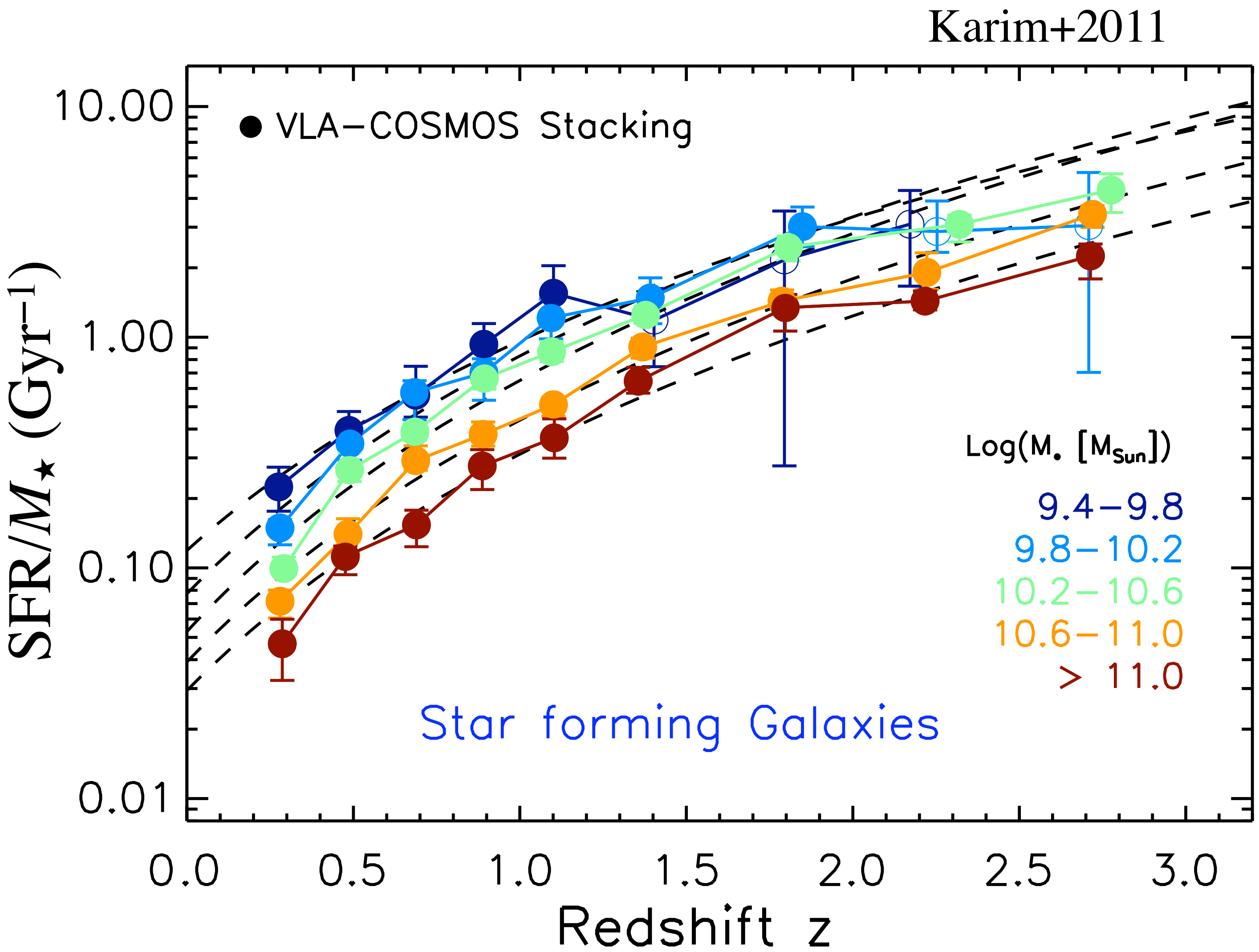

$$\frac{dN}{dM_\star dV}$$

Roughly constant values Schechter-function values M^* and faint-end slope α. Strong decrease in ϕ^* with z.

$$\frac{dM_\star}{d\mathrm{SFR}}$$

$\mathrm{SFR}/M_\star \propto M_\star^{-0.4} \times (1+z)^{3.5}$

Constraints on X-ray/SFR Relation in Universe

$$\frac{d\mathrm{SFR}}{dL_{\mathrm{X}}}$$

- To assess how the X-ray/SFR correlation evolves with redshift, we utilized the multiwavelength data to select galaxy populations in three SFR bins covering SFR = 1−100 $M_\odot$ yr^{-1} and the redshift range z = 0−3.
- Using the 4 Ms CDF-S data we performed X-ray stacking to measure population averaged X-ray luminosities and sensitively measure how L_X/SFR changes with redshift.

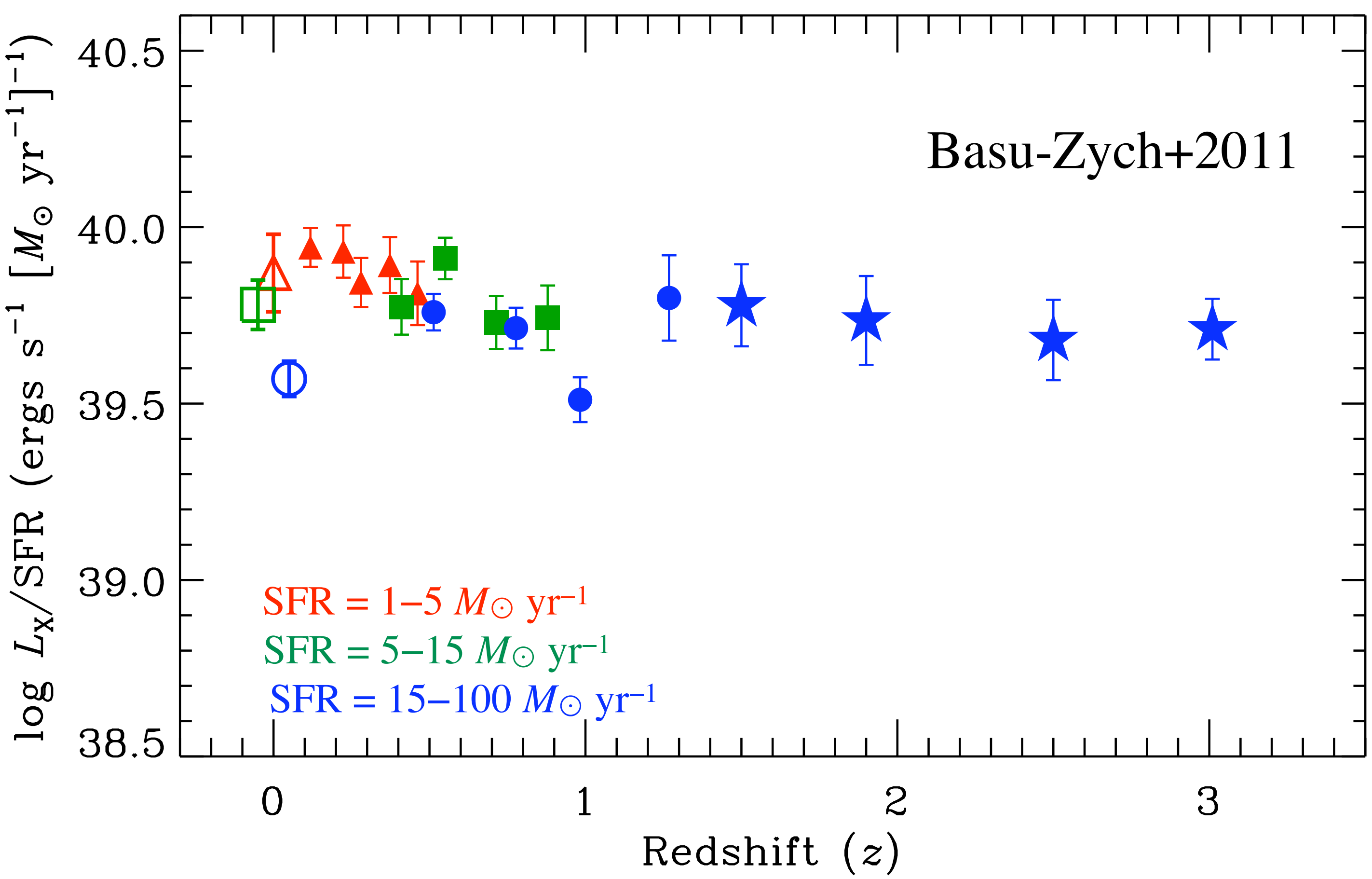

Constraints on X-ray/SFR Relation in Universe

$$\frac{d\mathrm{SFR}}{dL_\mathrm{X}}$$

- To assess how the X-ray/SFR correlation evolves with redshift, we utilized the multiwavelength data to select galaxy populations in three SFR bins covering SFR = 1−100 $M_\odot$ yr^{-1} and the redshift range z = 0−3.

- Using the 4 Ms CDF-S data we performed X-ray stacking to measure population averaged X-ray luminosities and sensitively measure how L_X/SFR changes with redshift.

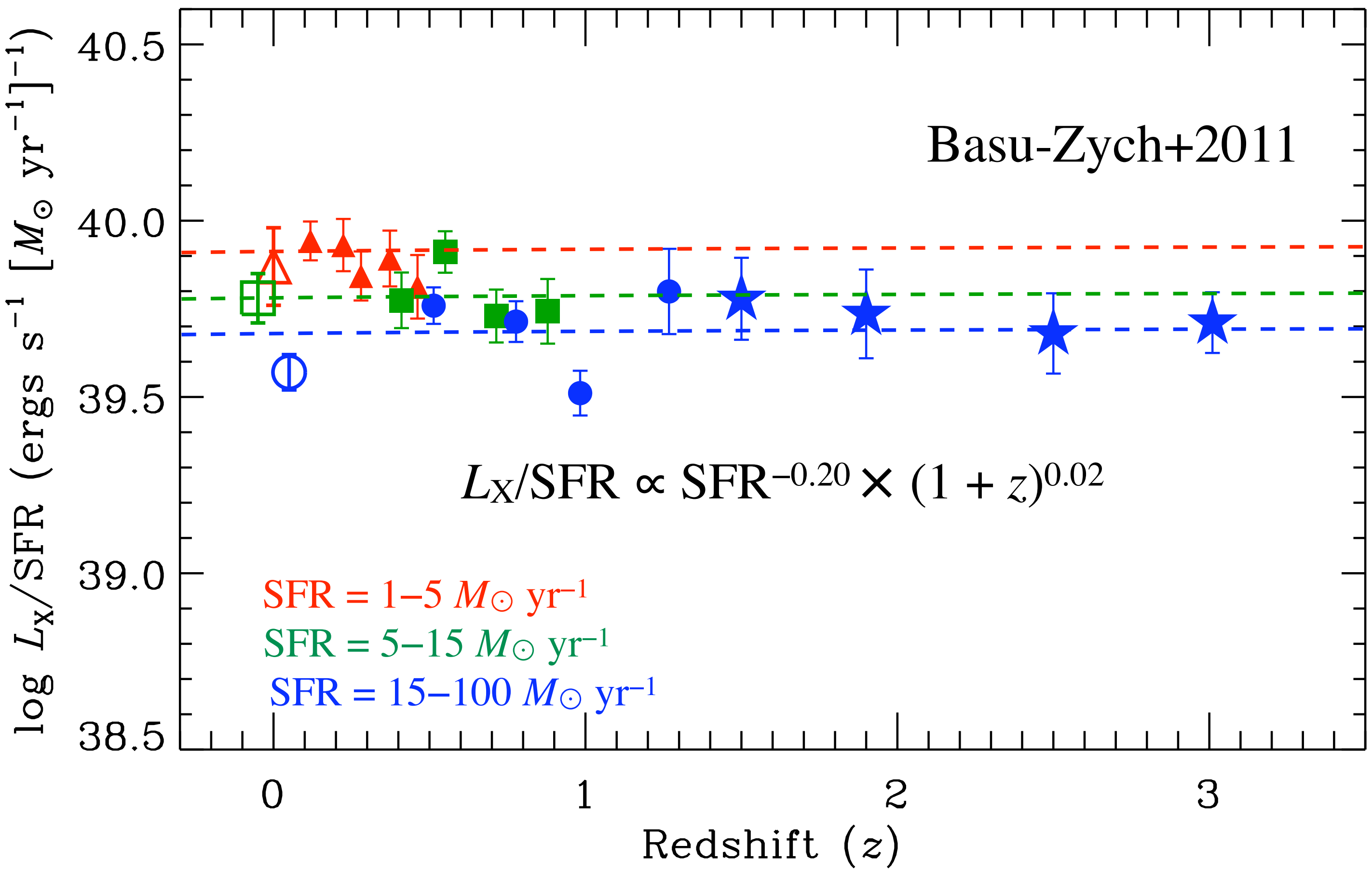

Constraints on X-ray/SFR Relation in Universe

$$\frac{d\mathrm{SFR}}{dL_\mathrm{X}}$$

- To assess how the X-ray/SFR correlation evolves with redshift, we utilized the multiwavelength data to select galaxy populations in three SFR bins covering SFR = 1−100 $M_\odot$ yr^{-1} and the redshift range z = 0−3.
- Using the 4 Ms CDF-S data we performed X-ray stacking to measure population averaged X-ray luminosities and sensitively measure how L_X/SFR changes with redshift.

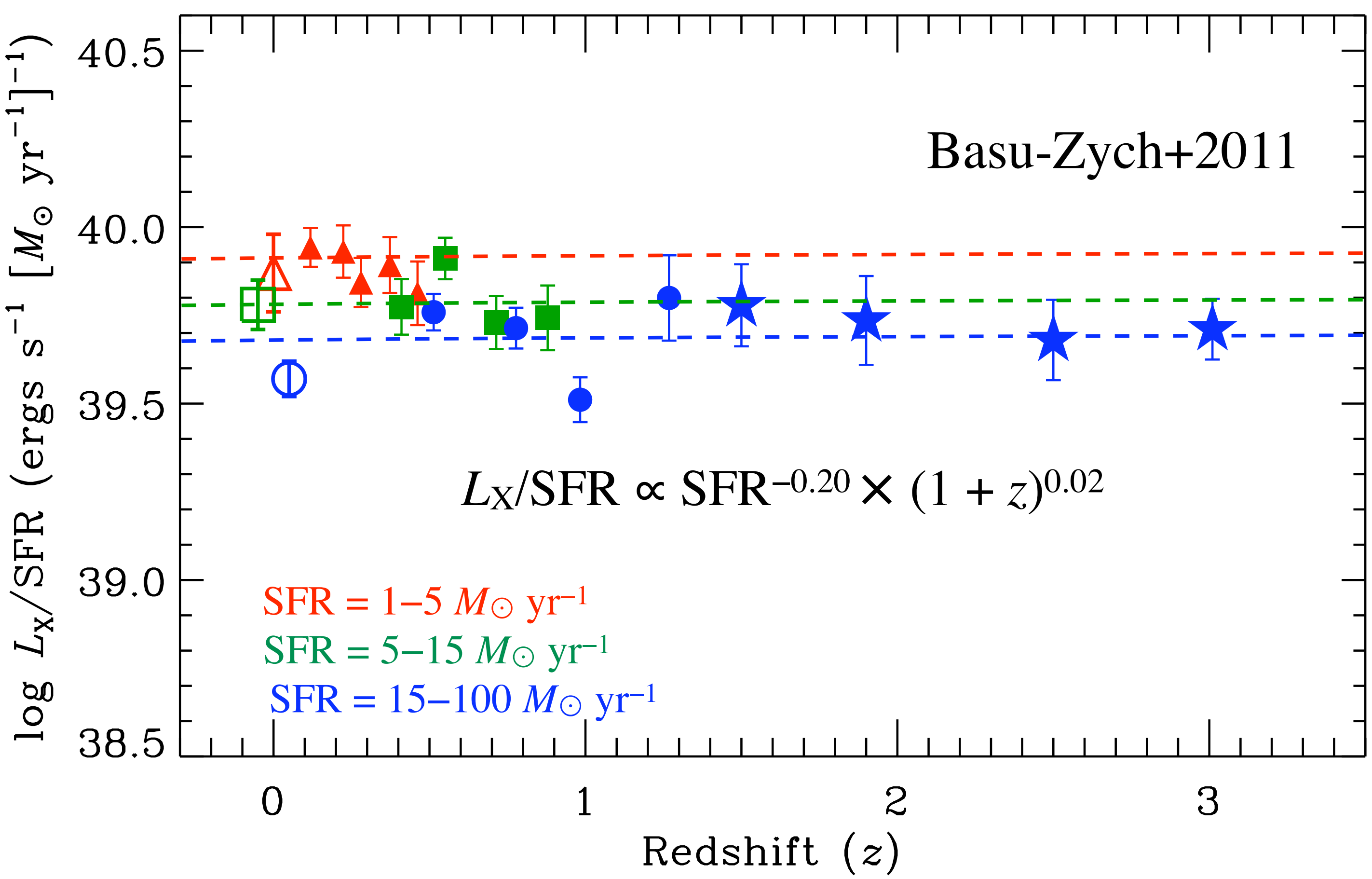

Local Galaxies

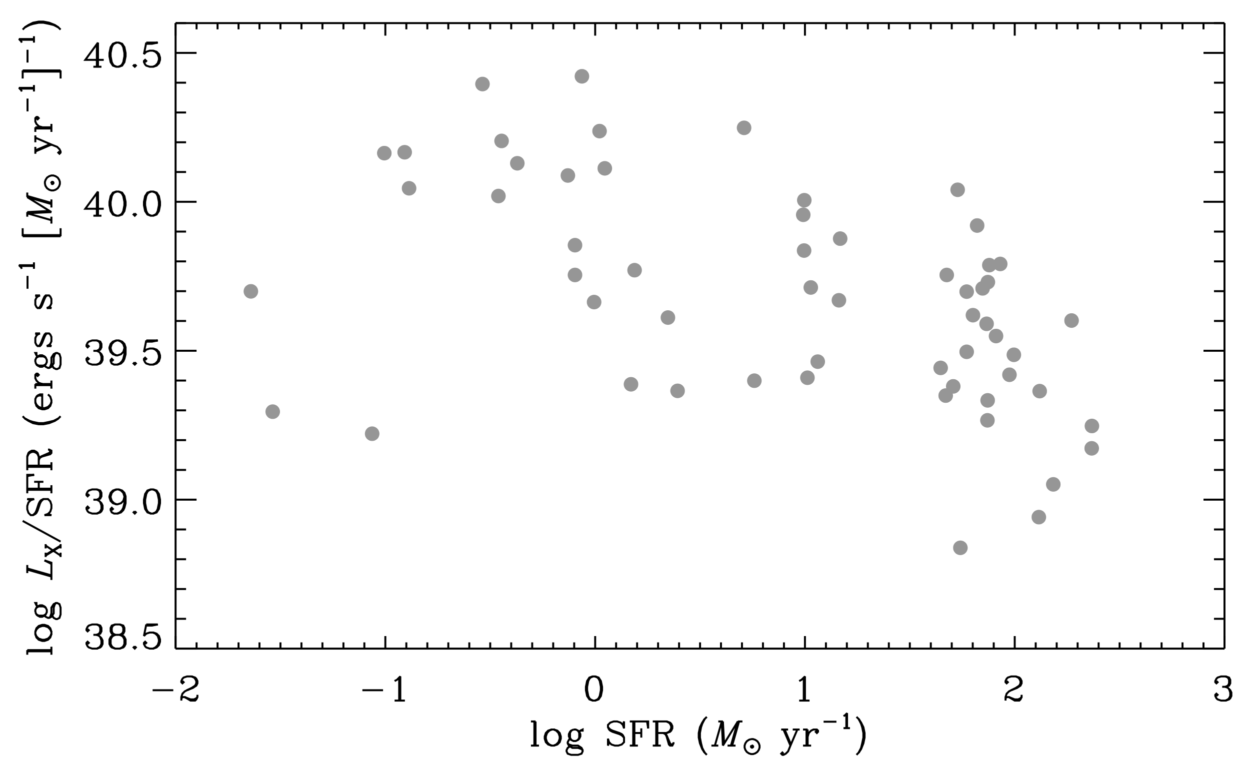

Colbert+2004; Iwasawa+2009; Lehmer+2010

Constraints on X-ray/SFR Relation in Universe

$$\frac{d\mathrm{SFR}}{dL_\mathrm{X}}$$

- To assess how the X-ray/SFR correlation evolves with redshift, we utilized the multiwavelength data to select galaxy populations in three SFR bins covering SFR = 1−100 $M_\odot$ yr^{-1} and the redshift range z = 0−3.
- Using the 4 Ms CDF-S data we performed X-ray stacking to measure population averaged X-ray luminosities and sensitively measure how L_X/SFR changes with redshift.

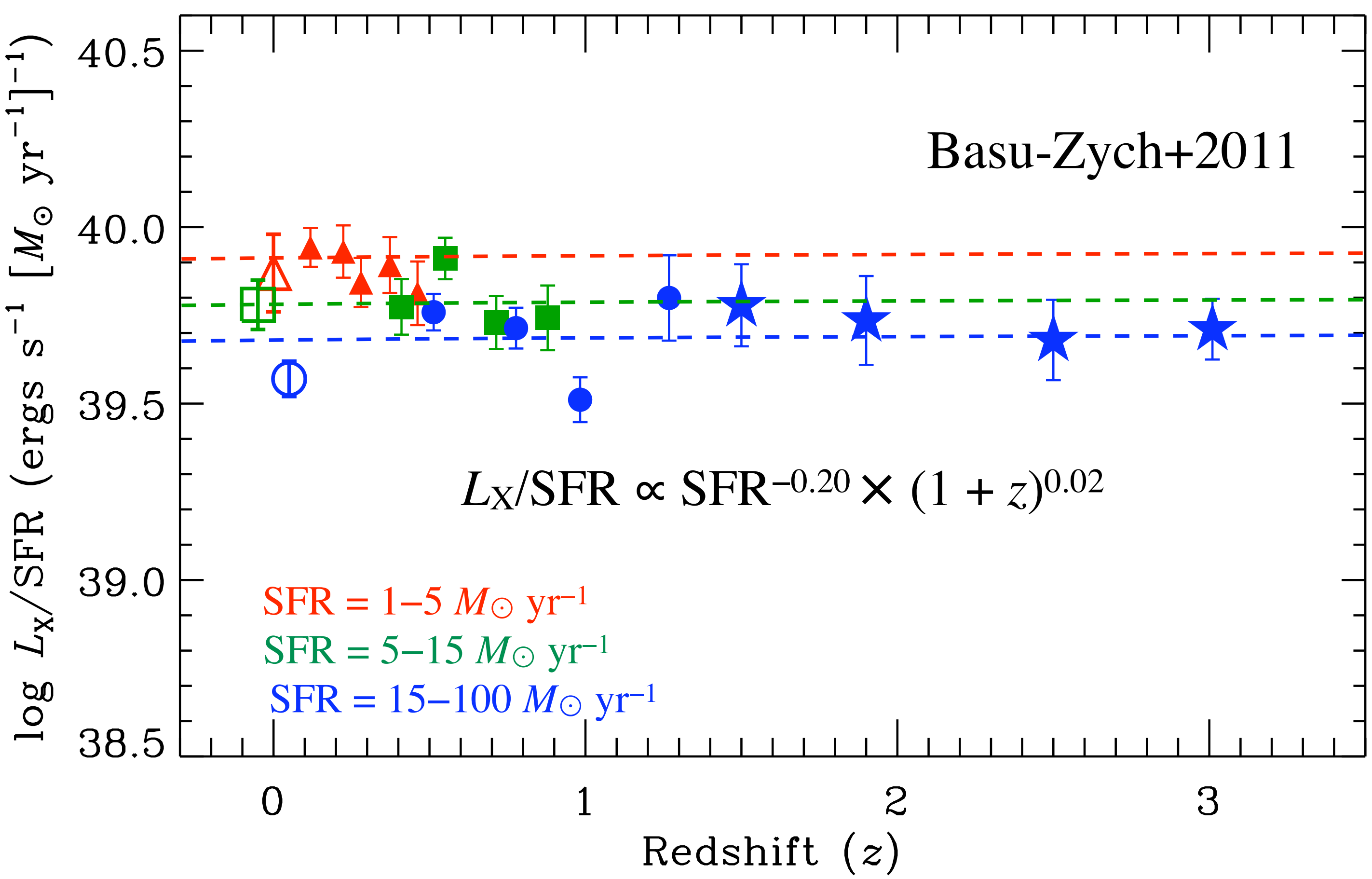

Local Galaxies

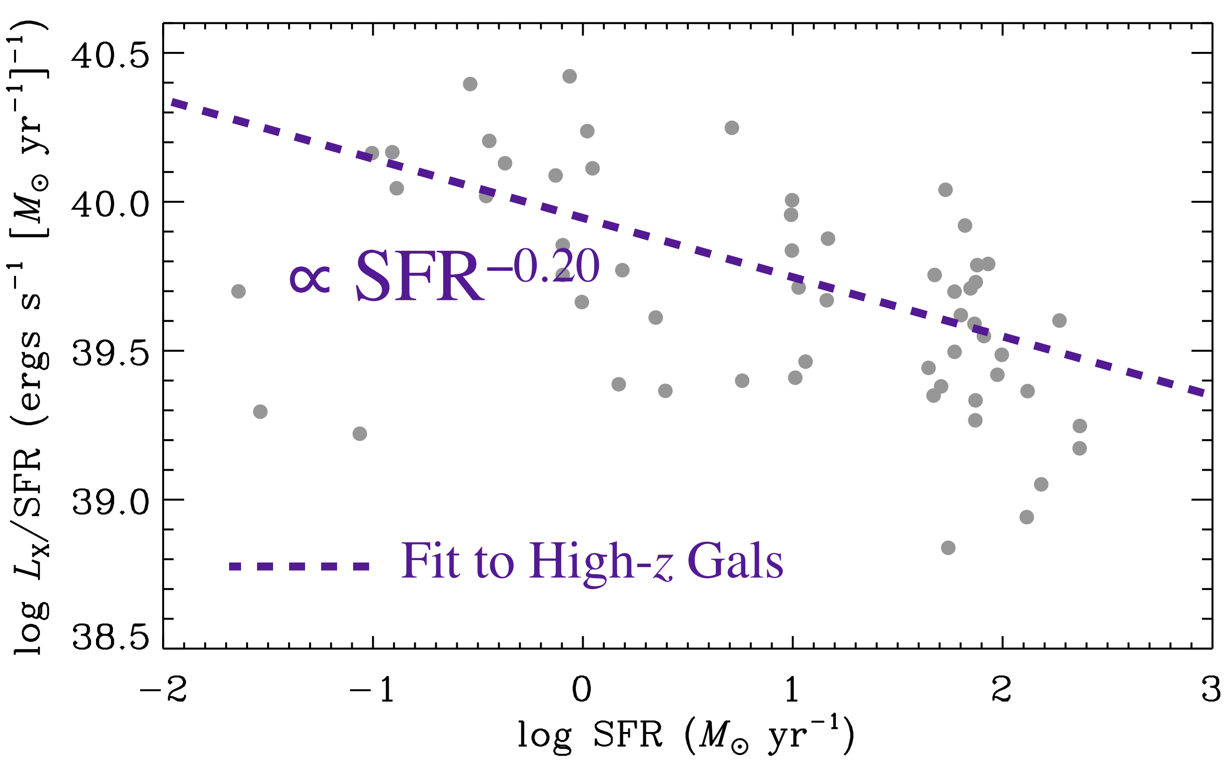

Colbert+2004; Iwasawa+2009; Lehmer+2010

Constraints on X-ray/SFR Relation in Universe

$$\frac{d\mathrm{SFR}}{dL_{\mathrm{X}}}$$

- To assess how the X-ray/SFR correlation evolves with redshift, we utilized the multiwavelength data to select galaxy populations in three SFR bins covering SFR = 1−100 $M_\odot$ yr^{-1} and the redshift range z = 0−3.
- Using the 4 Ms CDF-S data we performed X-ray stacking to measure population averaged X-ray luminosities and sensitively measure how L_X/SFR changes with redshift.

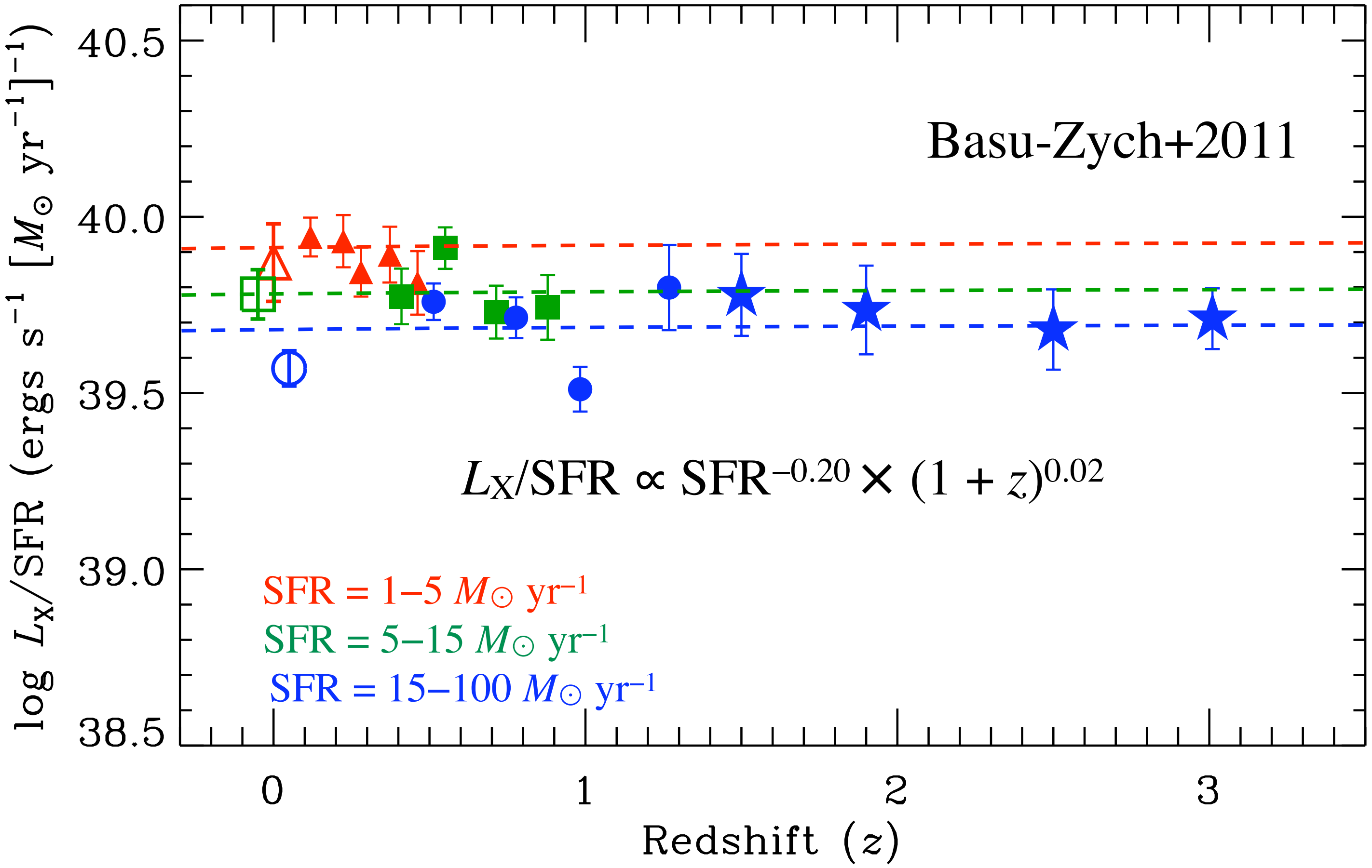

Local Galaxies

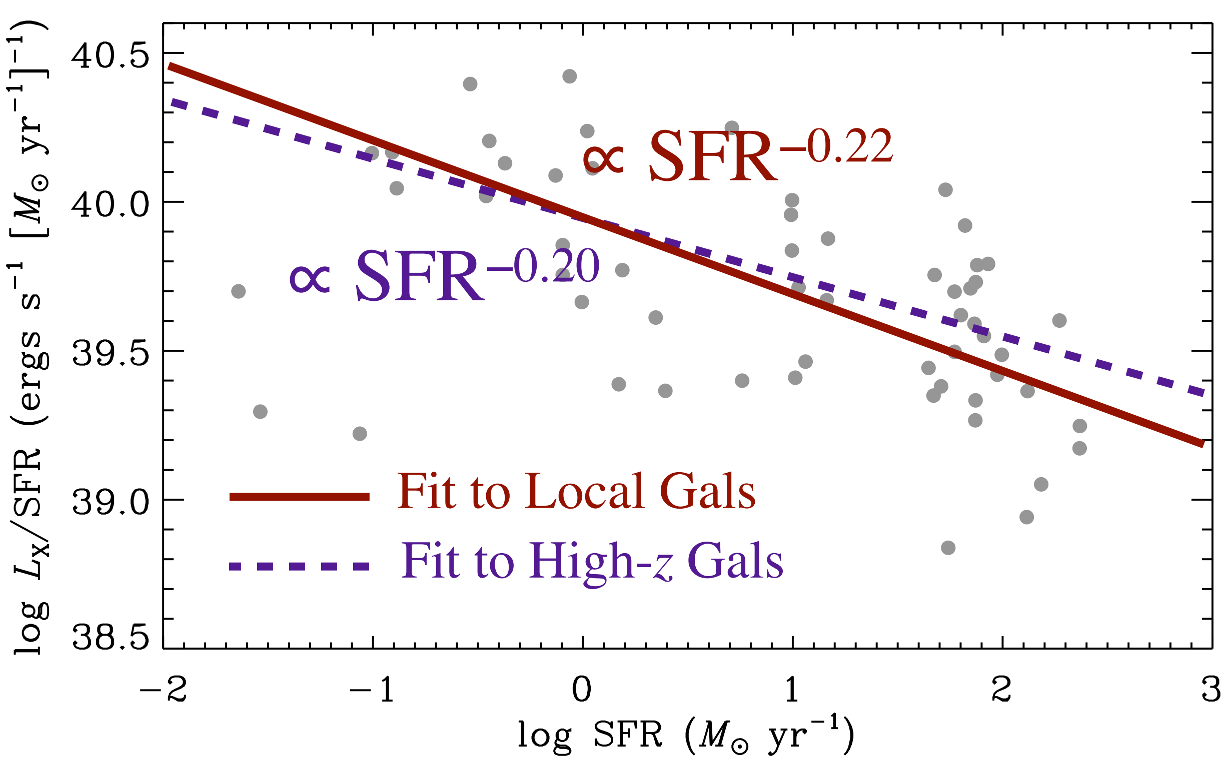

Colbert+2004; Iwasawa+2009; Lehmer+2010

Star-Forming Galaxy Number Counts

$$N(>S_X) = \frac{1}{\Omega_{\rm sky}} \int_{\infty}^{S_X} \left(\int_0^{\infty} \frac{dN}{dL_X dV} \frac{dL_X}{dS_X} \frac{dV}{dz} dz \right) dS_X$$

$$\frac{dN}{dL_X dV} = \frac{dN}{dM_\star dV} \frac{dM_\star}{d{\rm SFR}} \frac{d{\rm SFR}}{dL_X}$$

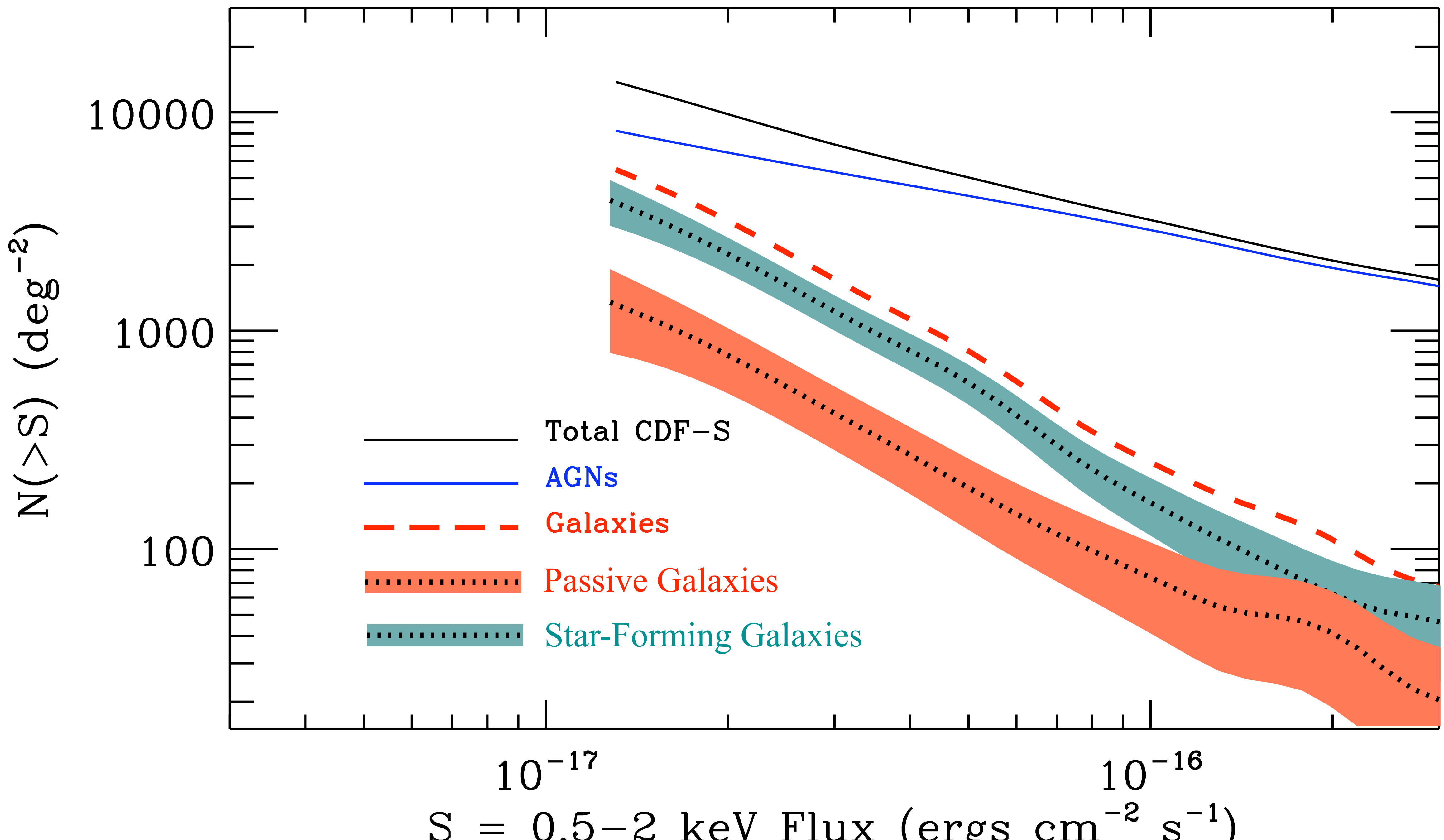

Star-Forming Galaxy Number Counts

$$N(>S_X) = \frac{1}{\Omega_{sky}} \int_{\infty}^{S_X} \left(\int_0^{\infty} \frac{dN}{dL_X dV} \frac{dL_X}{dS_X} \frac{dV}{dz} dz \right) dS_X$$

$$\frac{dN}{dL_X dV} = \frac{dN}{dM_\star dV} \frac{dM_\star}{d\mathrm{SFR}} \frac{d\mathrm{SFR}}{dL_X}$$

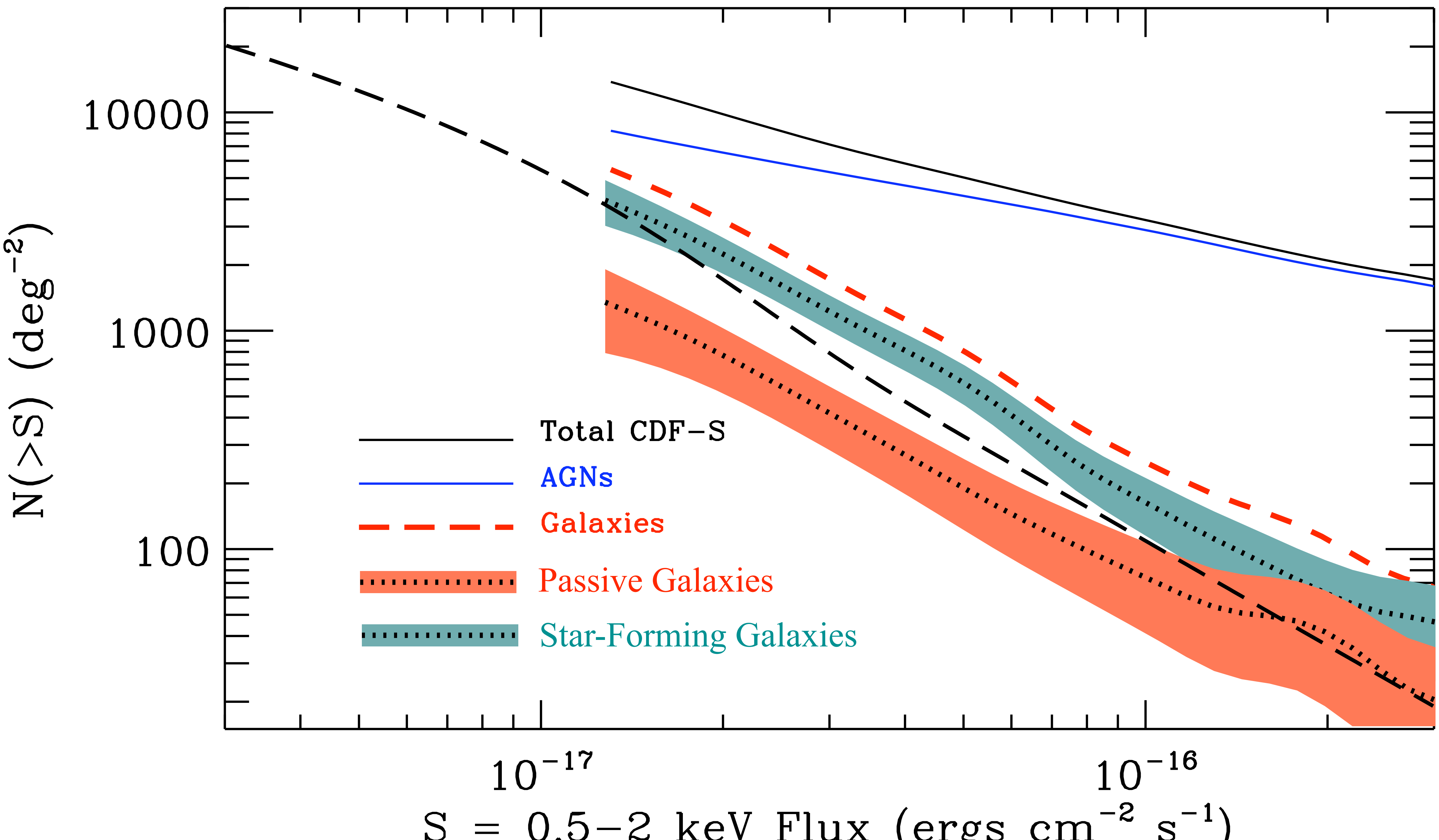

Star-Forming Galaxy Number Counts

$$N(>S_{\rm X}) = \frac{1}{\Omega_{\rm sky}} \int_{\infty}^{S_{\rm X}} \left(\int_0^{\infty} \frac{dN}{dL_{\rm X} dV} \frac{dL_{\rm X}}{dS_{\rm X}} \frac{dV}{dz} dz \right) dS_{\rm X}$$

$$\frac{dN}{dL_{\rm X} dV} = \frac{dN}{dM_{\star} dV} \frac{dM_{\star}}{d{\rm SFR}} \frac{d{\rm SFR}}{dL_{\rm X}}$$

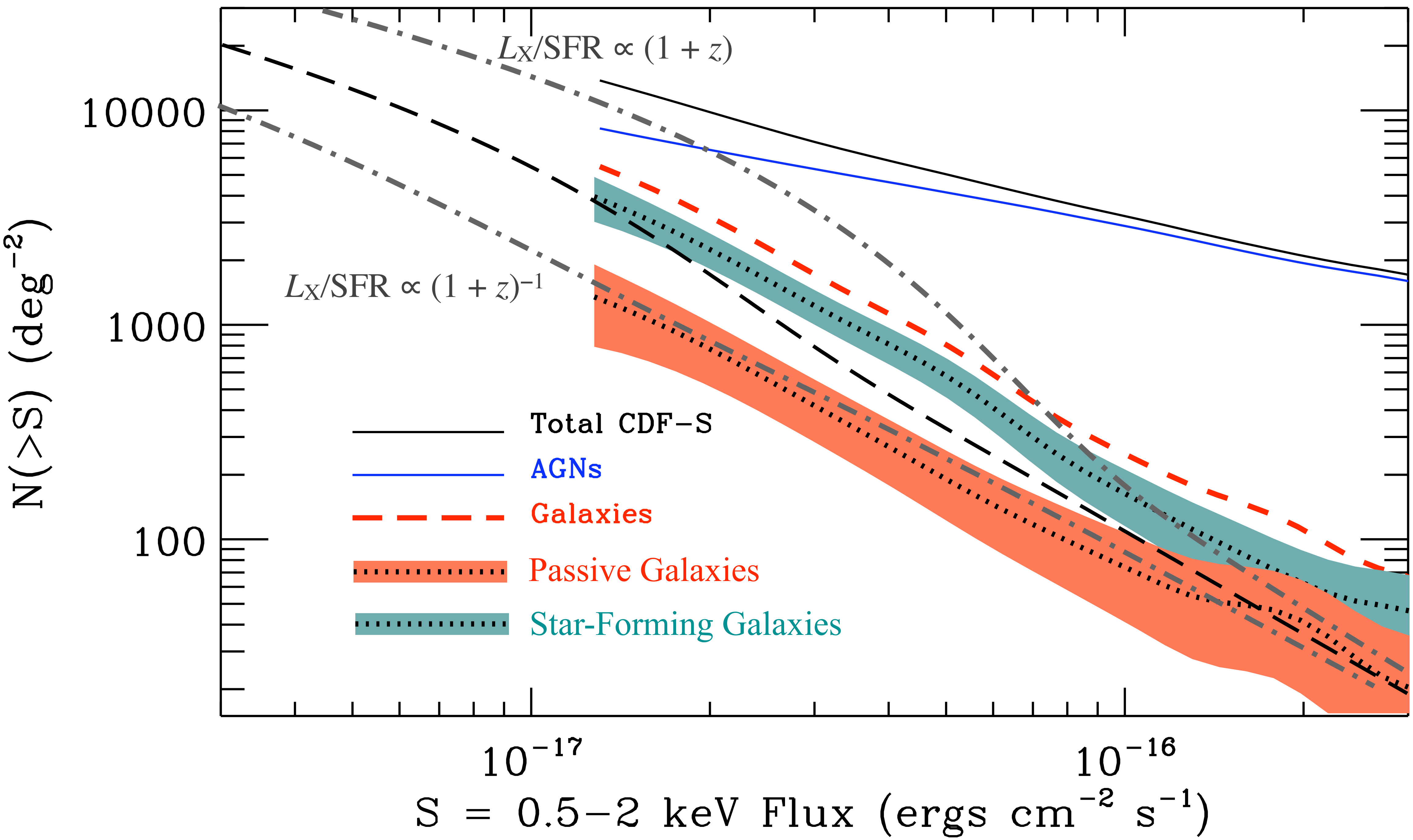

Conclusions

• The 4 Ms CDF-S have shown that the normal galaxy population rises quickly in source density at the faintest flux levels and make up ~40% of the normal galaxy number counts at 0.5−2 keV fluxes above 1.1×10^{-17} ergs cm^{-2} s^{-1}.

• The increase in galaxy number counts is largely driven by star-forming galaxies with passive early-type galaxies playing a small role.

• Stacking of normal galaxy populations selected by SFR show that the X-ray/SFR correlation holds out to $z \sim 3$.

• The combination of the observed evolution of the stellar mass function, the relationship between stellar mass and SFR, and the non-evolution of the X-ray/SFR correlation provide a reasonable prediction for the cumulative number counts observed in the 4 Ms CDF-S.